

1 **Whole genome sequencing of a wild yam species *Dioscorea tokoro* reveals a genomic
2 region associated with sex**

4 Satoshi Natsume¹, Hiroki Yaegashi¹, Yu Sugihara², Akira Abe¹, Motoki Shimizu¹, Kaori Oikawa¹,
5 Benjamen White³, Aoi Kudoh², Ryohei Terauchi^{1,2*}

7 ¹ Iwate Biotechnology Research Center, Kitakami, Iwate, 024-0003, Japan

8 ² Laboratory of Crop Evolution, Kyoto University, Mozume, Muko, Kyoto, 617-0001, Japan

9 ³ Earlham Institute, Norwich NR4 7UZ, United Kingdom

11 *Correspondence to Ryohei Terauchi (terauchi@ibrc.or.jp)

13 **Abstract**

15 *Dioscorea tokoro* is a wild species distributed in East Asia including Japan. Typical of the genus
16 *Dioscorea*, *D. tokoro* is dioecious with male and female flowers borne on separate individuals. To
17 understand its sex determination system and to serve as a model species for population genomics of
18 obligate outcrossing wild species, we set out to determine the whole genome sequence of the species.
19 Here we show 443 Mb genome sequence of *D. tokoro* distributed over 2,931 contigs that were
20 anchored on 10 linkage groups. Linkage analysis of sex in a segregating F1 family revealed a sex
21 determination locus residing on Pseudochromosome 3 with XY-type male heterogametic sex
22 determination system.

25 **key words**

27 (Keywords. *Dioscorea*, yam, dioecy, genome, sex determination.)

29 **Introduction**

31 The genus *Dioscorea* belongs to the monocotyledons and has 450 - 600 species distributed mainly in
32 tropical and subtropical area of the world (Coursey, 1972; Sugihara et al. 2021). Cultivated species of
33 *Dioscorea* are collectively called yam, which includes Guinea yam (*D. rotundata*) of West Africa
34 accounting for more than 90% of the world yam production (FAOSTAT, 2018). The entire genus of
35 *Dioscorea* is characterized by dioecy, with male and female flowers borne on separate individuals.
36 Consequently, the species of *Dioscorea* have obligate outcrossing, resulting in a higher level of
37 heterozygosity and frequent inter-species hybridization (Terauchi et al. 1992; Chaïr et al. 2010, 2016;

38 Girma et al. 2014; Scarcelli et al. 2006, 2017; Siadjeu et al. 2018; Sugihara et al. 2020, 2021; Bredeson
39 et al. 2022). Previously we reported the whole genome sequence of *D. rotundata* with 570 Mb in size
40 (Tamiru et al. 2017), which served as a reference to study population genomics of *D. rotundata* and
41 its wild relatives to reveal the origin of Guinea yam (Scarcelli et al. 2019; Sugihara et al. 2020).

42 *Dioscorea tokoro* is a wild species belonging to the section Stenophora. It is widely
43 distributed in East Asia including Japan. *D. tokoro* is a diploid species with a chromosome number $2n$
44 = $2x = 20$. It is a perennial species with rhizomes. In spring, shoots emerge from rhizomes and develop
45 to vines that twine around nearby trees in an anti-clockwise direction which expand alternate leaves
46 (Fig 1). The species commonly occurs along the fringes of forests in Japan. Crossing experiment is
47 easy and the generation time is relatively short (1-2 years), so that the species has been serving as a
48 model species of *Dioscorea*. The species was subjected to studies of population genetics (Terauchi
49 1990 : Terauchi and Konuma 1994; Terauchi et al. 1997), linkage mapping and elucidation of sex
50 determination mechanisms (Terauchi and Kahl, 2004).

51 To serve as a platform for future genomics study of the species, we here report the whole
52 genome sequence of *D. tokoro*. We combined Oxford Nanopore long read sequences and Illumina
53 short read sequences for de novo assembly to generate contigs. The contigs were further anchored on
54 linkage maps to generate pseudochromosomes. RNA-seq data were used for gene prediction. A
55 putative locus involved in *D. tokoro* sex determination was identified on Pseudochromosome 3.

56

57 **Results**

58

59 **Estimation of size of *D. tokoro* genome by flow cytometry**

60

61 We used a *D. tokoro* individual Kita1 collected at Kitakami, Iwate, Japan as well as *D. rotundata*
62 accession TDR96-F1 with known genome size (~570 Mb, Tamiru et al. 2017), as the material for flow
63 cytometry (FCM) analysis using nuclei prepared from fresh leaf samples. DNA of isolated nuclei were
64 stained with propidium iodide and analyzed by a flow cytometer. The value of G1 peak mean of *D.*
65 *tokoro* was 206.5, whereas that of *D. rotundata* was 303.6. The ratio between the two species was 0.68
66 (206.5/303.6). From these values the genome size of *D. tokoro* was estimated to be ~388 Mb (570 Mb
67 × 0.68) (Fig. S1).

68

69 **Reference assembly using Oxford Nanopore Technology**

70

71 Genomic DNA was extracted from fresh leaves of *D. tokoro* Kita1 and subjected to Oxford Nanopore
72 Technologies (ONT) sequencing. As a result, we obtained a total of 2,515,235 reads amounting 27.4
73 Gb in size (Table S1). We also performed Illumina sequencing of 35 - 251 bp read-length (total 24.6

74 Gb; obtained by MiSeq) as well as 150 bp read-length (total 37.8 Gb; obtained by HiSeq4000) (**Table**
75 **S2**). We assembled ONT reads and Illumina sequence reads using a hybrid assembler MaSuRCA
76 v3.3.4 (Zimin et al. 2013) with Flye assembler v2.6 (Kolmogorov et al. 2019) running internally,
77 which generated *D. tokoro* draft genome sequence consisting of 2,931 contigs amounting 443.5 Mb
78 with N_{50} being 586,368 bp (**Table 1**). The estimated genome size by k -mer analysis of the reads was
79 438.7 Mb. These estimated genome size based on DNA sequencing were larger than 388 Mb as
80 estimated by the FCM analysis.

81

82 **Anchoring of contigs on *D. tokoro* linkage maps**

83 To generate *D. tokoro* pseudochromosomes, we mapped the contigs on ten linkage groups. For this
84 purpose, we crossed a female individual Waka1 (P1) with a male individual Kita1 (P2) to obtain F1
85 progeny comprising 186 individuals (**Fig. S2**; **Table S3**). These plants were genotyped by RAD
86 markers (**Fig. S3**; Baird et al, 2008). We identified 946 SNPs and 180 presence/absence
87 polymorphisms (PAs) that are heterozygous in P1 and homozygous in P2 parents, and 724 SNPs and
88 880 PAs that are homozygous in P1 and heterozygous in P2 parents (**Table S4**). These DNA markers
89 were used for construction of linkage map using pseudo-testcross approach (Grattapaglia and Sederoff,
90 1994). We obtained two linkage maps, one for DNA markers heterozygous in P1 parent, and the other
91 for markers heterozygous in P2 parent (**Fig. S4**). Since each RAD marker has ~75 bp sequence, this
92 information was used to associate RAD marker to contigs generated by the de novo assembly (**Fig.**
93 **S5**). This method allowed us to anchor contigs amounting 378.8 Mb (85.4% of the total genome size)
94 to the linkage maps (**Table S5**) and to combine the two linkage groups and generate
95 pseudochromosomes 1-10 with sizes ranging from 31.5 Mb (Pseudochromosome 5) to 54.6 Mb
96 (Pseudochromosome 1) (**Fig. 2**).

97 BUSCO analysis (Mosè et al. 2020) showed that complete BUSCO value of 98%, indicating
98 that our *D. tokoro* genome sequence is of a sufficient quality as the reference (**Table 1**).

99

100 **Gene prediction**

101

102 We performed RNA-seq of 18 samples representing different organs and developmental stages of *D.*
103 *tokoro* (**Table S6**). The total size of RNA-seq reads amounted 31.17 Gb. These RNA-seq reads were
104 mapped to the contigs, revealing a total of 29,084 genes, among which 25,447 genes were assigned to
105 pseudochromosomes (**Table 2**).

106

107 **Sex determination in *D. tokoro***

108

109 The 186 F1 progeny derived from a cross between Waka1 female (P1) and Kita1 male (P2) parents
110 segregated in 38 female, 89 male, and 59 non-flowering in 2011 (**Table S3**). We attempted to identify
111 genomic region that shows association with sex of the F1 individuals. As a result of Fisher's exact test
112 based on the sex and genotype contingency table of each progeny, we found a significant association
113 of the middle position of Pseudochromosome 3 with sex when the DNA markers heterozygous in the
114 male parent (P2) were used. By contrast, there was no association detected if we use the markers
115 heterozygous in the female parent (P1; **Fig. 3**). This result indicates a male heterogametic sex
116 determination (XY) system in *D. tokoro*, and supports our previous analysis with AFLP markers
117 (Terauchi and Kahl, 1999).

118

119 Discussion

120

121 Here we report *D. tokoro* draft genome sequence of 443.5 Mb in size. For the species of the genus
122 *Dioscorea*, whole genome sequences are available for *D. rotundata* (Tamiru, 2017; Sugihara et al.
123 2020), *D. dumetorum* (Siadjeu et al. 2020) and *D. alata* (Bredeson et al. 2022). Genome sizes of these
124 species were 570 Mb (*D. rotundata*), 485 Mb (*D. dumetorum*) and 480 Mb (*D. alata*). The genome of
125 *D. tokoro* is slightly smaller than the genomes of *Dioscorea* species so far reported.

126 Basic chromosome number of *Dioscorea* is suggested to be ten. *D. tokoro* revealed to have ten
127 linkage groups in this study, which is in line with the report of linkage group obtained by AFLP
128 analysis (Terauchi and Kahl, 1999). It is contrasting to *D. rotundata* ($2n = 2x = 40$) and *D. alata* ($2n$
129 = $2x = 40$), both belonging to the section *Enantiophyllum*. It is likely that during the evolution of
130 *Dioscorea*, chromosome duplication occurred. However, no signature of genome duplication observed
131 in *D. rotundata* genome (Tamiru et al. 2017), suggesting that genome duplication happened in a
132 remote past.

133 Sex determination of *D. tokoro* was confirmed to be XY type male heterogametic system. It is
134 similar to the XY system in *D. alata* (Cormier et al. 2019), but in contrast to ZW female heterogametic
135 system in *D. rotundata* (Tamiru et al. 2017). It is likely that sex determination locus has shifted
136 multiple times in the genus. Future study will identify the genes involved in *D. tokoro* sex
137 determination.

138 In summary, we determined a draft genome sequence of a wild yam species *D. tokoro*. This
139 chromosome level sequence information will serve as a platform to understand population genomics
140 of this obligate outcrossing species and to elucidate the mechanism and evolution of its sex
141 determination system.

142

143 **Materials and Methods**

144

145 **Plant Materials**

146

147 A female plant, Waka1 (original code: DT49) (**Fig. S2A; Fig. S2D**), was collected from Tahara,
148 Wakayama Pref. in Central Japan. A male plant, Kita1 (original code: 110628-5), was collected from
149 Waga-Sennin of Iwate Pref. in Northern Japan (**Fig. S2B; Fig. S2D**). To construct a linkage map, we
150 obtained F1 seeds derived from a cross between Waka1 (P1) and Kita1 (P2) in 2011. We started
151 growing 206 F1 individuals in 2012 and obtained sex data for 186 F1 individuals in 2014 and 2015
152 (**Fig. S2C**).

153

154 **Flow cytometry**

155

156 Flow cytometry (FCM) analysis was carried out using nuclei prepared from fresh leaf samples. Nuclei
157 were isolated and stained with propidium iodide (PI) and analyzed using a Cell Lab QuantaTM SC
158 Flow Cytometer (Beckman Coulter, USA) following the manufacturer's protocol.

159

160 **Whole genome sequencing and *de novo* assembly**

161

162 To generate *Dioscorea tokoro* reference genome sequence, we sequenced the male plant Kita1 using
163 the PromethION sequencer (Oxford Nanopore Technologies). First, Kita1 DNA was extracted from
164 fresh leaves as described in our previous report (Tamiru et al., 2017). The extracted DNA was
165 subjected to size selection and purification with a gel extraction kit (Large Fragment DNA Recovery
166 Kit; Zymo Research). Finally, the purified DNA was sequenced by PromethION at GeneBay company,
167 Yokohama, Japan (<http://genebay.co.jp>). As the first step for genome assembly, we removed the
168 lambda phage genome from Nanopore fastq using NanoLyse 1.1.0 (De Coster et al. 2018) and filtered
169 out reads with an average read quality score less than seven and those shorter than 1,000 bases with
170 Nanofilt v2.2 (De Coster et al. 2018). We also performed two types of Illumina sequencing, 251 bp
171 paired-end sequencing using MiSeq and 150 bp paired-end sequencing using HiSeq4000. Next, we
172 assembled the filtered long DNA sequence reads with the hybrid assembler MaSuRCA v3.3.4 (Zimin
173 et al. 2013), run internally by Flye assembler v2.6 (Kolmogorov et al. 2019).

174

175 **Assessing genome completeness**

176

177 To evaluate the completeness of the gene set in the assembled genome, we applied BUSCO analysis
178 (Bench-Marking Universal Single Copy) v5.1.2 (Mosè et al. 2020). We used the default gene search

179 method 'metaeuk gene search' instead of the traditional gene search method using AUGUSTUS (Hoff
180 and Stanke, 2013) and TBLASTN (Camacho et al. 2009). We set "genome" as the assessment mode
181 and used embryophyte_odb10 as the lineage datasets.

182

183 **Gene prediction and annotation**

184

185 For gene prediction, we used RNA-seq data from 18 samples of *D. tokoro*, representing seven organs
186 of Kita1 individual (leaves, stems, root apex, rhizome bud, rhizome root, rhizome stem, and rhizome
187 storage) and 11 different flowering stages in female and male *D. tokoro* plants from the wild (**Table**
188 **S6**). First, according to the manufacturer's instructions, total RNAs were used to construct cDNA
189 libraries using a TruSeq RNA Sample Prep Kit V2 (Illumina, USA). Then, the bulked cDNA library
190 was sequenced using the Illumina NextSeq500 platform for 75 bp single-end reads. In the fastq quality
191 control step, we first remove adapters, poly(A), and the reads shorter than 50 bp using FaQCs (Lo and
192 Chain, 2014). Subsequently, we removed low-quality bases from the read end (window size = 5, base
193 quality average = 20) and low-quality reads with an average read quality below 20 using PRINSEQ
194 lite 0.20.4 (Schmieder and Edwards, 2011). Quality trimmed reads were aligned to the assembled
195 genome with HISAT2 v2.1 (Kim et al. 2019) with the options "--max-intronlen 15000 --dta". Next,
196 transcript alignments were assembled with StringTie v1.3.6 (Pertea et al. 2015) separately for each
197 BAM file. Finally, these GFF files were integrated with TACO v0.7.3 (Niknafs et al. 2017) with the
198 option "--filter-min-length 90", generating 24,148 gene models within the assembled genome (**Table**
199 **2**). Additionally, 34,539 peptide sequences that were predicted in *D. rotundata* genome (Tamiru et al.,
200 2017) [ENSEMBL (http://plants.ensembl.org/Dioscorea_rotundata/Info/Index).] were aligned to
201 assembled genome with Spaln2 v2.3.3 (Iwata and Gotoh, 2012). Consequently, 1,900 CDSs that did
202 not overlap with the new gene models were added to the new gene models (**Table 2**). In addition, the
203 3,036 transcripts that were assembled in the StringTie program but rejected in the TACO program
204 were added manually. Finally, gene models shorter than 75 bases were removed, and InterProScan
205 v5.36 (N) was used to predict ORFs (open reading frames) and strand information for each gene model.
206 We predicted 29,084 genes, including 54,847 transcript variants (**Table 2**). For gene annotation, the
207 predicted gene models were searched in the Pfam protein family database using InterProScan (Blum
208 et al. 2021) and with the blastx command in BLAST+ (Camacho et al. 2009) with the option "--eval
209 1e-10", using the Viridiplantae database from UniProt as the target database. The resulting gene
210 models and annotations were uploaded to <https://genome-e.ibrc.or.jp/resource/dioscorea-tokoro/>.

211

212 **Identification of parental line-specific heterozygous markers**

213

214 ***RAD sequencing***

215 We performed RAD-seq to develop the linkage map as previously described (Tamiru et al., 2017).
216 Genomic DNA was extracted from fresh leaves of Waka1, Kita1, and 186 F1 individuals and digested
217 with the restriction enzymes PacI and NlaIII to prepare libraries used to generate 75-bp paired-end
218 reads by Illumina NextSeq500. We remove adapters and the unpaired reads using FaQCs and
219 PRINSEQ lite as previously described. The filtered RAD-seq reads were used as RAD-tags (**Fig. S3**).
220

221 ***SNP-type heterozygous markers***

222 RAD-tags were aligned to the assembled genome of *D. tokoro* in this study using BWA (ver. 0.7.12).
223 SNP-based genotypes for P1, P2, and F1 individuals was obtained as a variant call format (VCF) file.
224 The VCF file was generated from BAM files of P1, P2, and F1 individuals using SAMtools (ver 1.5),
225 and the VCF variants were called and filtered using BCFtools (ver 1.5). As a result, 5,894 P1- or P2-
226 heterozygous SNP markers were selected (shown as “All RAD markers” in **Table S4**). Next, to
227 increase the accuracy of the selected markers, their segregation (1:1 ratio) was confirmed in F1
228 individuals obtained from a cross between P1 and P2. If the segregation ratio was out of the confidence
229 interval ($P < 0.001$) hypothesized by the binomial distribution, B (n = number of individuals, $P = 0.5$),
230 the markers were excluded from further analysis. Finally, 3,057 P1-heterozygous SNP markers and
231 1,559 P2-heterozygous SNP markers were selected (shown as “Confirmed segregation ratio” in **Table**
232 **S4**). Additional details are provided in the **Supplementary Method**.
233

234 ***Presence/absence-type heterozygous markers***

235 The presence/absence-type markers were defined based on the alignment depth of parental line RAD-
236 tags. The presence/absence-type markers were called by the following method: First, the VCF file was
237 generated from BAM files of P1 and P2 and selected the region where either P1 or P2 had sufficient
238 read depth (≥ 8) and that the other parental line had no read depth in that region. Next, BEDtools (ver
239 2.26) converted continuous positions in the VCF file to a feature, and only sufficiently wide features
240 (width ≥ 50 bp) were retained as the BED file. For these regions in the BED file, the F1 individual’s
241 genotypes were classified into three categories (depth ≥ 3 , depth = 0, others) and three genotypes
242 (“presence,” “absence,” “NA”). As a result, 5,071 PA markers were selected (shown as “All RAD
243 markers” in **Table S4**). We then applied the same binomial test as for the SNP-type heterozygous
244 markers. Finally, 480 P1-heterozygous PA markers and 1,682 P2-heterozygous PA markers were
245 selected (shown as “Confirmed segregation ratio” in **Table S4**). Additional details are provided in the
246 **Supplementary Method**.
247

248 ***Integration of SNP-type and presence/absence-type heterozygous markers.***

249

250 We integrated SNP-type and PA-type heterozygous markers to develop parental line-specific linkage
251 maps. Two types of markers were defined: P1-heterozygous markers and P2-heterozygous markers.
252 If an SNP-type marker was heterozygous in P1 but homozygous in P2 or if a PA-type marker was
253 present in P1 and absent in P2, it was classified as a P1-heterozygous marker set. Conversely, if a
254 SNP-type marker was homozygous and heterozygous in P1 and P2, respectively, or if a PA-type
255 marker was absent in P1 but present in P2, it was classified as a P2-heterozygous marker set.
256

257 **Linkage maps construction**

258

259 ***Pruning and flanking markers by Spearman's correlation coefficients***

260 Pairwise matrix of Spearman's correlation coefficients (ρ) were calculated for every marker pair in
261 each contig in each marker set (P1-heterozygous marker set and P2-heterozygous marker set).
262 According to the histogram of absolute ρ calculated from each contig, most markers on the same
263 contigs were correlated with each other. Therefore, we pruned correlated flanking markers to remove
264 redundant markers. Finally, we obtained 2,818 markers for linkage mapping (shown as "Pruning and
265 flanking" in **Table S4**).
266

267 ***Linkage mapping***

268 We converted the flanking markers obtained as described in the previous section into the genotype-
269 formatted data for constructing genetic linkage maps using MSTmap (Wu, 2008) with following
270 parameter sets: "populationtype DH; distancefunction kosambi; cutoffpvalue 0.000000000001;
271 nomapdist 15.0; nomapsize 0; missingthreshold 25.0; estimationbeforeclustering no; detectbaddata
272 no; objective_function ML" for P1-heterozygous marker set and P2-heterozygous marker set. After
273 trimming the orphan linkage groups, we solved the complemented-phased duplex linkage groups
274 caused by coupling-type and repulsion-type markers in the pseudo-testcross method. Finally, two
275 parental-specific linkage maps were constructed. These two linkage maps were designated as P1-map
276 (constructed using P1-heterozygous marker set) and P2-map (constructed using P2-heterozygous
277 marker set) (**Fig. S4A**; **Fig. S4C**). The order and names of each linkage group were organized
278 according to the P2-map (**Fig. S4** and **Fig. S5**). The linkage groups were visualized by R/qtl (Broman
279 et al., 2003).
280

281 **Generation of pseudochromosomes**

282

283 Based on a matrix derived from the contigs shared between the P1- and P2-maps, i.e., linkage groups
284 (**Fig. S5**), the contigs were anchored and linearly ordered as pseudochromosomes. First, we identified
285 contigs whose markers were allocated to different linkage groups during the anchoring and ordering

286 process. Such contigs were further divided into sub-contigs to ensure that they were not allocated to
287 wrong pseudochromosomes. Next, we divided the contigs at the proper positions as described
288 previously (Tamiru et al. 2017). Finally, we followed the described method (Tamiru et al. 2017) to
289 generate ten pseudochromosomes.

290

291 **Identification of sex associated region**

292

293 To identify the sex-associated genomic region, we performed Fisher's exact test using the genotype
294 of 127 F1 individuals based on 2,730 markers located on the pseudochromosomes (**Table S4**) and
295 their sex phenotype (**Table S3**). Fisher's exact test was performed using the fisherexact function in
296 the python SciPy package. A significance threshold of 5% false discovery rate (FDR) was calculated
297 using the multipletests function in the python statsmodels package with the option method="fdr_bh"
298 (Benjamini / Hochberg procedure).

299

300

301 **Data Availability**

302

303 All sequencing read data generated for this work have been deposited at the DNA Databank of Japan
304 (DDBJ) database under BioProject PRJDB12945; see **Table S1** and **S2** for individual sample
305 accession numbers. The genomic sequence file (fasta), gene annotation file (gff3), and gene/protein
306 sequences file (fasta) are available at the following URL: <https://genome-e.ibrc.or.jp/resource/dioscorea-tokoro/>

307

308

309

310 **Funding**

311

312 This work was supported by Iwate Biotechnology Research Center.

313

314

315 **Disclosures**

316

317 The authors have no conflicts of interest to declare.

318

319

320 **Acknowledgments**

321

322 We dedicate this work to Günter Kahl, a pioneer of *Dioscorea* molecular genetics. In this research
323 work we used the NIG supercomputer at ROIS National Institute of Genetics, and the supercomputer
324 of ACCMS, Kyoto University.

325

326

327 **References**

328

329 Beck, H. E., Zimmermann, N. E., McVicar, T. R., Vergopolan, N., Berg, A., and Wood, E. F. (2018)
330 Present and future Köppen-Geiger climate classification maps at 1-km resolution. Scientific
331 data, 5.1: 1-12.

332

333 Blum, M., Chang, H. Y., Chuguransky, S., Grego, T., Kandasamy, S., Mitchell, A., Gift N., et al.
334 (2021) The InterPro protein families and domains database: 20 years on. Nucleic acids
335 research, 49.D1: D344-D354.

336

337 Bredeson, J. V., Lyons, J. B., Oniyinde, I. O., Okereke, N. R., Kolade, O., Nnabue, I., Nwadili, C. O.,
338 et al. (2022) Chromosome evolution and the genetic basis of agronomically important traits
339 in greater yam. Nature communications, 13.1: 1-16.

340

341 Broman, K. W., Wu, H., Sen, Š., and Churchill, G. A. (2003) R/qtl: QTL mapping in experimental
342 crosses. bioinformatics, 19.7: 889-890.

343

344 Burkhill, I. H. (1960) The organography and the evolution of Dioscoreaceae, the family of the yams.
345 Journal of the Linnean Society, 56: 319-412.

346

347 Camacho, C., Coulouris, G., Avagyan, V., Ma, N., Papadopoulos, J., Bealer, K., and Madden, T. L.
348 (2009) BLAST+: architecture and applications. BMC bioinformatics, 10.1: 1-9.

349

350 Chaïr, H., Cornet, D., Deu, M., Baco, M. N., Agbangla, A., Duval, M. F., and Noyer, J. L. (2010)
351 Impact of farmer selection on yam genetic diversity. Conservation Genetics. 11.6: 2255-2265.

352

353 Chaïr, H., Sardos, J., Supply, A., Mournet, P., Malapa, R., and Lebot, V. (2016) Plastid phylogenetics
354 of Oceania yams (*Dioscorea* spp., Dioscoreaceae) reveals natural interspecific hybridization
355 of the greater yam (*D. alata*). Botanical Journal of the Linnean Society. 180.3: 319-333.

356

- 357 Cormier, F., Lawac, F., Maledon, E., Gravillon, M.-C., Nudol, E., Mournet, P., Vignes H, et al. (2019)
358 A reference high-density genetic map of greater yam (*Dioscorea alata* L.). *Theor Appl Genet.*
359 132: 1733–1744.
- 360
- 361 Danecek, P., Bonfield, J. K., Liddle, J., Marshall, J., Ohan, V., Pollard, M. O., Andrew W., et al.
362 (2021) Twelve years of SAMtools and BCFtools. *Gigascience*, 10.2: giab008.
- 363
- 364 De Coster, W., D'Hert, S., Schultz, D. T., Cruts, M., and Van Broeckhoven, C. (2018) NanoPack:
365 visualizing and processing long-read sequencing data. *Bioinformatics*, 34.15: 2666-2669.
- 366
- 367 FAOSTAT (2018) Food and Agriculture Organization. <http://www.fao.org/statistics>.
- 368
- 369 Girma, G., Hyma, K. E., Asiedu, R., Mitchell, S. E., Gedil, M., and Spillane, C. (2014) Next-
370 generation sequencing based genotyping, cytometry and phenotyping for understanding
371 diversity and evolution of guinea yams. *Theoretical and Applied Genetics*. 127.8: 1783-1794.
- 372
- 373 Grattapaglia, D., and Sederoff, R. (1994) Genetic linkage maps of *Eucalyptus grandis* and *Eucalyptus*
374 *urophylla* using a pseudo-testcross: mapping strategy and RAPD markers. *Genetics*, 137.4:
375 1121-1137.
- 376
- 377 Hoff, K. J., and Stanke, M. (2013). WebAUGUSTUS—a web service for training AUGUSTUS and
378 predicting genes in eukaryotes. *Nucleic acids research*, 41.W1: W123-W128.
- 379
- 380 Iwata, H., and Gotoh, O. (2012) Benchmarking spliced alignment programs including Spaln2, an
381 extended version of Spaln that incorporates additional species-specific features. *Nucleic acids*
382 *research*, 40.20: e161-e161.
- 383
- 384 Kim, D., Paggi, J. M., Park, C., Bennett, C., and Salzberg, S. L. (2019) Graph-based genome alignment
385 and genotyping with HISAT2 and HISAT-genotype. *Nature biotechnology*, 37.8: 907-915.
- 386
- 387 Kolmogorov, M., Yuan, J., Lin, Y., and Pevzner, P. A. (2019) Assembly of long, error-prone reads
388 using repeat graphs. *Nature biotechnology*, 37.5: 540-546.
- 389
- 390 Li, H. (2013) Aligning sequence reads, clone sequences and assembly contigs with BWA-MEM. *arXiv*
391 preprint arXiv:1303.3997.
- 392

- 393 Lo, C. C., and Chain, P. S. G. (2014) Rapid evaluation and quality control of next generation
394 sequencing data with FaQCs. *BMC Bioinformatics*. 15: 366.
- 395
- 396 Mosè M., Matthew R. B., Mathieu S., Felipe A. S., and Evgeny M. Z., (2021) BUSCO Update: Novel
397 and Streamlined Workflows along with Broader and Deeper Phylogenetic Coverage for
398 Scoring of Eukaryotic, Prokaryotic, and Viral Genomes, *Molecular Biology and Evolution*,
399 Volume 38, Issue 10, Pages 4647-4654.
- 400
- 401 Niknafs, Y. S., Pandian, B., Iyer, H. K., Chinnaiyan, A. M., and Iyer, M. K. (2017) TACO produces
402 robust multisample transcriptome assemblies from RNA-seq. *Nature methods*, 14.1: 68-70.
- 403
- 404 Okagami, N. and Kawai, M. (1982) Dormancy in *Dioscorea*: Differences of temperature responses in
405 seed germination among six Japanese species. *The botanical magazine= Shokubutsu-gaku-*
406 *zasshi*. Tokyo. 95.2: 155-166.
- 407
- 408 Oyama, M., Tokiwano, T., Kawaii, S., Yoshida, Y., Mizuno, K., Oh, K., et al. (2017) Protodioscin,
409 Isolated from the Rhizome of *Dioscorea tokoro* Collected in Northern Japan is the Major
410 Antiproliferative Compound to HL-60 Leukemic Cells. *Current bioactive compounds*. 13.2:
411 170-174.
- 412
- 413 Pertea, M., Pertea, G. M., Antonescu, C. M., Chang, T. C., Mendell, J. T., and Salzberg, S. L. (2015)
414 StringTie enables improved reconstruction of a transcriptome from RNA-seq reads. *Nature*
415 *biotechnology*, 33.3: 290-295.
- 416
- 417 Quinlan, A. R., and Hall, I. M. (2010) BEDTools: a flexible suite of utilities for comparing genomic
418 features. *Bioinformatics*, 26.6: 841-842.
- 419
- 420 Scarcelli, N., Tostain, S., Vigouroux, Y., Agbangla, C., Daïnou, O., and Pham, J. L. (2006) Farmers'
421 use of wild relative and sexual reproduction in a vegetatively propagated crop. The case of
422 yam in Benin. *Molecular Ecology*. 15.9: 2421-2431.
- 423
- 424 Scarcelli, N., Chaïr, H., Causse, S., Vesta, R., Couvreur, T. L. P., and Vigouroux, Y. (2017) Crop wild
425 relative conservation: Wild yams are not that wild. *Biological Conservation*. 210: 325-333.
- 426

- 427 Scarcelli, N., Cubry, P., Akakpo, R., Thuillet, A. C., Obidiegwu, J., Baco, M. N., Otoo, E., et al. (2019)
428 Yam genomics supports West Africa as a major cradle of crop domestication. *Science*
429 *advances*. 5.5: eaaw1947.
- 430
- 431 Schmieder, R., and Edwards, R. (2011) Quality control and preprocessing of metagenomic datasets.
432 *Bioinformatics*. 27.6: 863-864.
- 433
- 434 Siadjeu, C., Mayland-Quellhorst, E., and Albach, D. C. (2018) Genetic diversity and population
435 structure of trifoliate yam (*Dioscorea dumetorum* Kunth) in Cameroon revealed by
436 genotyping-by-sequencing (GBS). *BMC Plant Biology*. 18.1: 1-14.
- 437
- 438 Siadjeu, C., Pucker, B., Viehöver, P., Albach, D.C., and Weisshaar, B. (2020) High Contiguity de
439 novo Genome Sequence Assembly of Trifoliate Yam (*Dioscorea dumetorum*) Using Long
440 Read Sequencing. *Genes*. 11: 274.
- 441
- 442 Sugihara, Y., Darkwa, K., Yaegashi, H., Natsume, S., Shimizu, M., Abe, A., Hirabuchi, A., et al.
443 (2020) Genome analyses reveal the hybrid origin of the staple crop white Guinea yam
444 (*Dioscorea rotundata*). *Proceedings of the National Academy of Sciences*. 117.50: 31987-
445 31992.
- 446
- 447 Sugihara, Y., Kudoh, A., Oli, M. T., Takagi, H., Natsume, S., Shimizu, M., Abe, A., et al. (2021)
448 Population Genomics of Yams: Evolution and Domestication of *Dioscorea* Species. In:
449 Population Genomics. pp. 1-28. Springer, Cham.
- 450
- 451 Tamiru, M., Natsume, S., Takagi, H., White, B., Yaegashi, H., Shimizu, M., et al. (2017) Genome
452 sequencing of the staple food crop white Guinea yam enables the development of a molecular
453 marker for sex determination. *BMC biology*. 15.1: 1-20.
- 454
- 455 Terauchi, R. (1990) Genetic diversity and population structure of *Dioscorea tokoro* Makino, a
456 dioecious climber. *Plant Species Biology*, 5.2: 243-253.
- 457
- 458 Terauchi, R., Chikaleke, V. A., Thottappilly, G., and Hahn, S. K. (1992) Origin and phylogeny of
459 Guinea yams as revealed by RFLP analysis of chloroplast DNA and nuclear ribosomal DNA.
460 *Theoretical and Applied Genetics*. 83.6: 743-751.
- 461

- 462 Terauchi, R. and Konuma, A. (1994) Microsatellite polymorphism in *Dioscorea tokoro*, a wild yam
463 species. *Genome*, 37: 794-801.
- 464
- 465 Terauchi, R., Terachi, T., and Miyashita, N. T. (1997) DNA polymorphism at the Pgi locus of a wild
466 yam, *Dioscorea tokoro*. *Genetics*, 147.4: 1899-1914.
- 467
- 468 Terauchi, R. and Kahl, G. (1999) Mapping of the *Dioscorea tokoro* genome: AFLP markers linked to
469 sex. *Genome* 42: 752-762.
- 470
- 471 Terauchi, R. and Kahl, G. (2004) Sex determination in *Dioscorea tokoro*, a wild yam species. In *Sex*
472 *determination in plants* (pp. 165-174). Garland Science.
- 473
- 474 Wessel, P., Luis, J. F., Uieda, L., Scharroo, R., Wobbe, F., Smith, W. H. F., and Tian, D. (2019) The
475 Generic Mapping Tools version 6. *Geochemistry, Geophysics, Geosystems*, 20, 5556-5564.
476 <https://doi.org/10.1029/2019GC008515>
- 477
- 478 Wu, Y., Bhat, P. R., Close, T. J., and Lonardi, S. (2008) Efficient and accurate construction of genetic
479 linkage maps from the minimum spanning tree of a graph. *PLoS genetics*, 4.10: e1000212.
- 480
- 481 Zimin, A. V., Marçais, G., Puiu, D., Roberts, M., Salzberg, S. L., and Yorke, J. A. (2013) The
482 MaSuRCA genome assembler. *Bioinformatics*, 29.21: 2669-2677.
- 483
- 484
- 485

486 **Figures Legends**

487

488 **Fig. 1 Botanical characteristics of *Dioscorea tokoro*.** (A) *D. tokoro* is a herbaceous climber species.
489 Aerial stems twine around tree trunks. (B) Stem twines in an anti-clockwise direction (left-handed;
490 sinistrorse). Leaves alternate. (C) Leaf shape is usually heart-shaped. Leaf blades are typically 5-12
491 cm long and 5-12 cm wide. (D) Female pendulous inflorescences. (E) Close-up view of a female
492 flower. Three-locular ovary are below the petal. Three-lobed pistil and six degenerated stamens around
493 the pistil are seen. Petal apex is round and curled inward. (F) Male upright inflorescences. (G) Close-
494 up view of a male flower. Pedicel branches from the base and has a few flowers. Six stamens, and
495 degenerated pistil in the center. Petal apex is round and curled inward. The scale is same as (E). (H)
496 Female inflorescence with immature obovate-elliptic capsules. Capsules reflex and dehisce at maturity.
497 (I) Male inflorescence. The scale is same as (H). (J) Mature fruit has three capsules, with winged two

498 seeds placed alternately overlapped near its base. Seed's wing is biased wider toward capsule apex.
499 (K) Underground rhizome of *D. tokoto*. (L) A side view of the rhizome from a different angle. The
500 direction of the white arrow corresponds to (K).

501

502 **Fig. 2 An integrated linkage and physical map of *D. tokoro*.** Approximately 85.4% of the *D. tokoro*
503 contig sequences were anchored using a RAD-based genetic map generated with 186 F1 individuals
504 obtained from a cross between Waka1 (P1: female) and Kita1 (P2: male). The 10 pseudochromosomes
505 are numbered from chrom_01 to chrom_10. Markers are located according to genetic distance (cM).
506 The black frame in the center of each group represents the reconstructed pseudochromosome and
507 orange and green bars indicate P1-map and P2-map, respectively. Thin grey lines connecting linkage
508 map and pseudochromosome indicate the positions of markers. The blue dots indicate the positions of
509 PA markers.

510

511 **Fig. 3 Genome-wide association mapping of sex in the F1 progeny derived from a cross between**
512 **Waka1 (P1: female) and Kita1 (P2: male) in *D. tokoro*.** Manhattan plot of markers associated with
513 sex phenotype as determined by Fisher's exact test with (A) P1-heterozygous marker set and (B) with
514 P2-heterozygous marker set. Orange and blue dots indicate SNP and presence/absence markers,
515 respectively, showing significant association with sex based on a 5 % false discovery rate ($q < 0.05$).

516

517

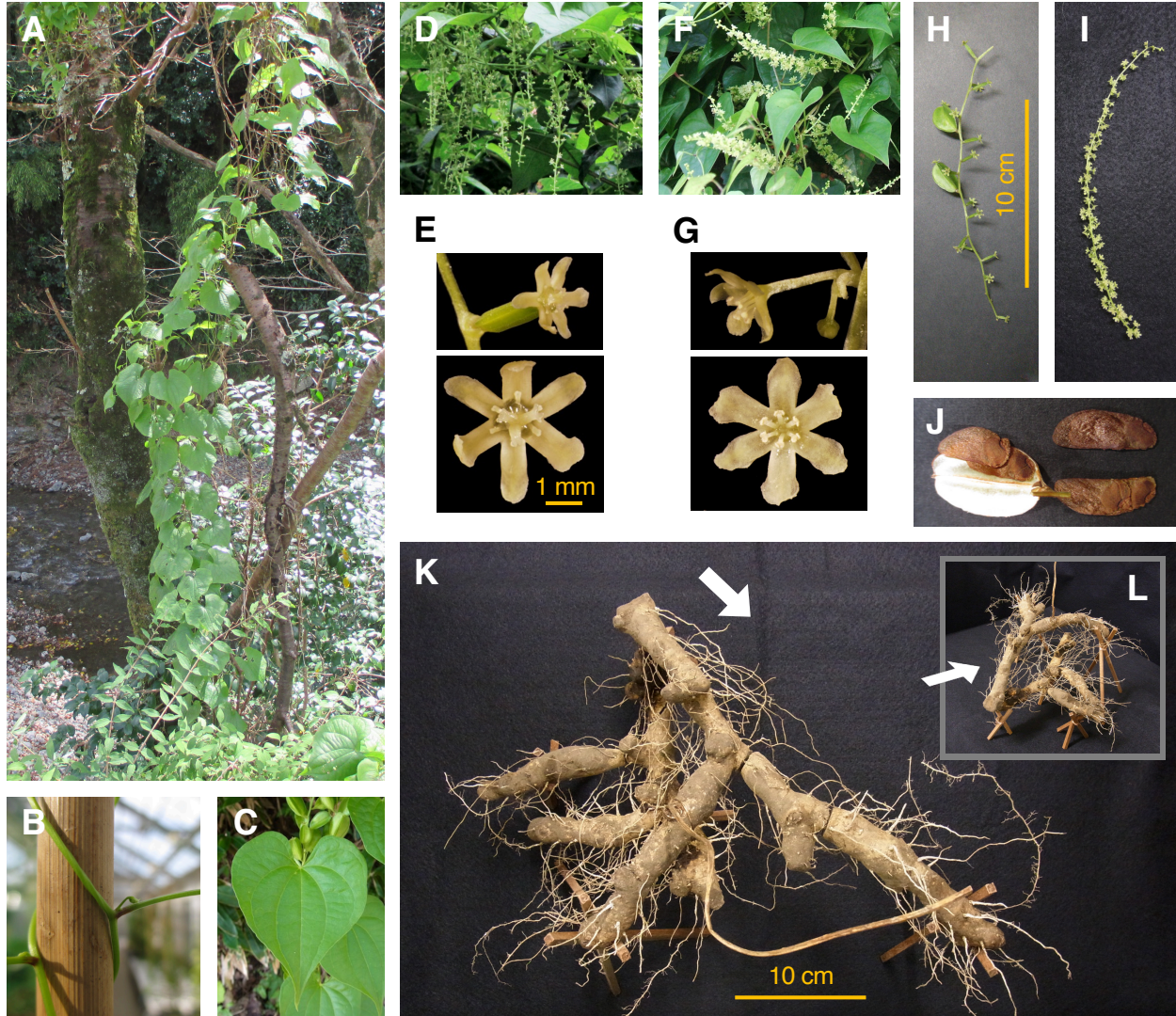


Fig. 1 Botanical characteristics of *Dioscorea tokoro*. (A) *D. tokoro* is a herbaceous climber species. Aerial stems twine around tree trunks. (B) Stem twines in an anti-clockwise direction (left-handed; sinistrorse). Leaves alternate. (C) Leaf shape is usually heart-shaped. Leaf blades are typically 5-12 cm long and 5-12 cm wide. (D) Female pendulous inflorescences. (E) Close-up view of a female flower. Three-locular ovary are below the petal. Three-lobed pistil and six degenerated stamens around the pistil are seen. Petal apex is round and curled inward. (F) Male upright inflorescences. (G) Close-up view of a male flower. Pedicel branches from the base and has a few flowers. Six stamens, and degenerated pistil in the center. Petal apex is round and curled inward. The scale is same as (E). (H) Female inflorescence with immature obovate-elliptic capsules. Capsules reflex and dehisce at maturity. (I) Male inflorescence. The scale is same as (H). (J) Mature fruit has three capsules, with winged two seeds placed alternately overlapped near its base. Seed's wing is biased wider toward capsule apex. (K) Underground rhizome of *D. tokoro*. (L) A side view of the rhizome from a different angle. The direction of the white arrow corresponds to (K).

Table 1. Summary of a reference genome of *D. tokoro* (Kita1).

Total number of contigs	2,931
Total base-pairs (bp)	443,501,147
Estimated genome size from k-mer (bp)	438,704,233
Average contig size (bp)	151,313
Longest contig (bp)	6,172,819
Shortest contig (bp)	502
N50 (bp)	586,368
Total BUSCO groups searched	1,614
Complete BUSCOs (%)	98.0
Complete and single-copy BUSCOs (%)	92.9
Complete and duplicated BUSCOs (%)	5.1
Fragmented BUSCOs (%)	1.1
Missing BUSCOs (%)	0.9

Table 2. Summary of predicted genes in the *D. tokoro* genome

	Contigs (2,931)	Pseudochrom. (01-10)
No. genes	29,084	25,447
(total transcript variant)	(54,847)	(48,271)
ORF status		
Complete	21,610	19,069
5' partial	195	166
3' partial	4,752	4,091
Internal	157	127
No ORF	2,370	1,994
Prediction software		
TACO	24,148	21,239
Spaln2	1,900	1,581
StringTie	3,036	2,627

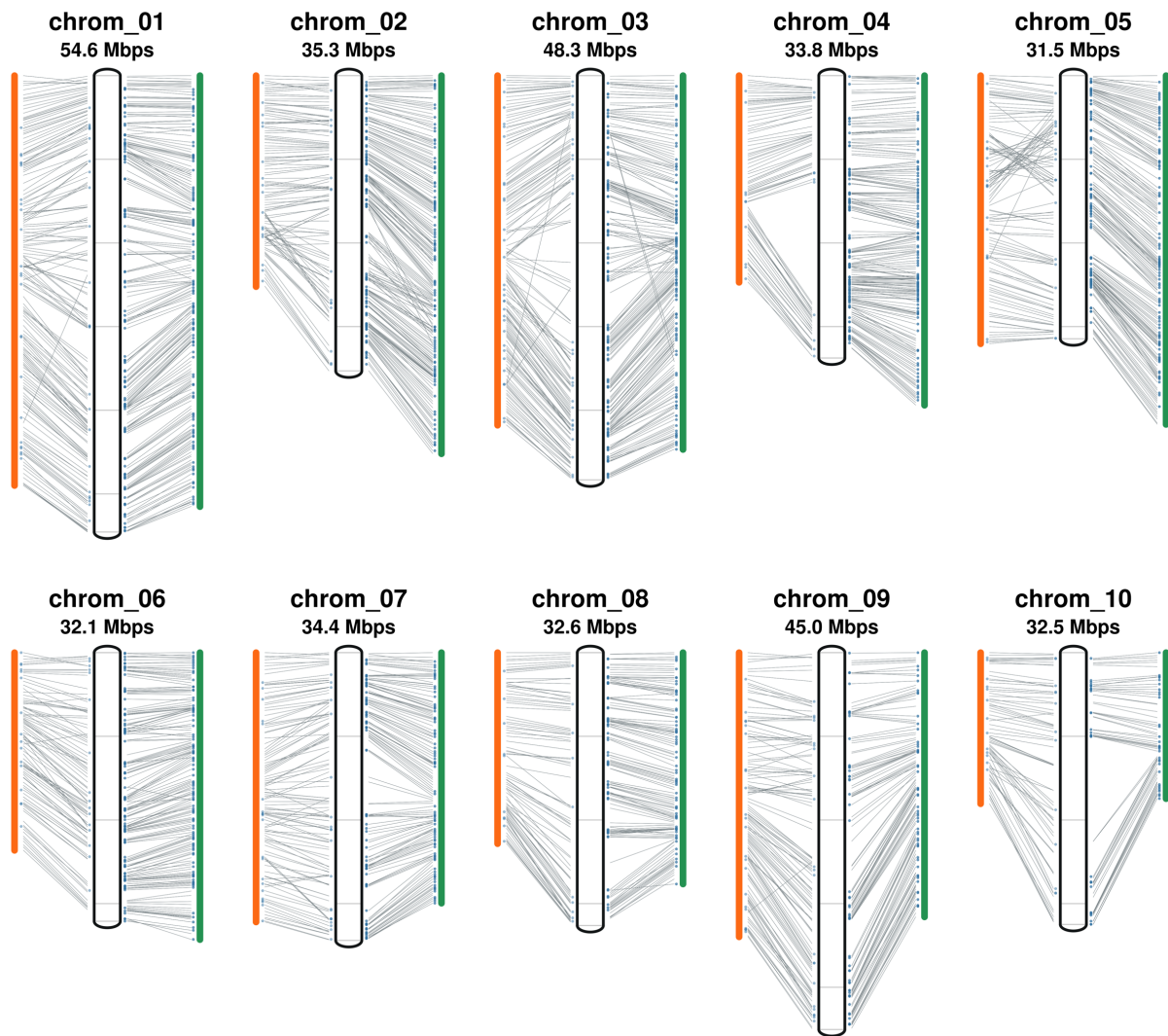


Fig. 2 An integrated linkage and physical map of *D. tokoro*. Approximately 85.4% of the *D. tokoro* contig sequences were anchored using a RAD-based genetic map generated with 186 F1 individuals obtained from a cross between Waka1 (P1: female) and Kita1 (P2: male). The 10 pseudochromosomes are numbered from chrom_01 to chrom_10. Markers are located according to genetic distance (cM). The black frame in the center of each group represents the reconstructed pseudochromosome and orange and green bars indicate P1-map and P2-map, respectively. Thin grey lines connecting linkage map and pseudochromosome indicate the positions of markers. The blue dots indicate the positions of PA markers.

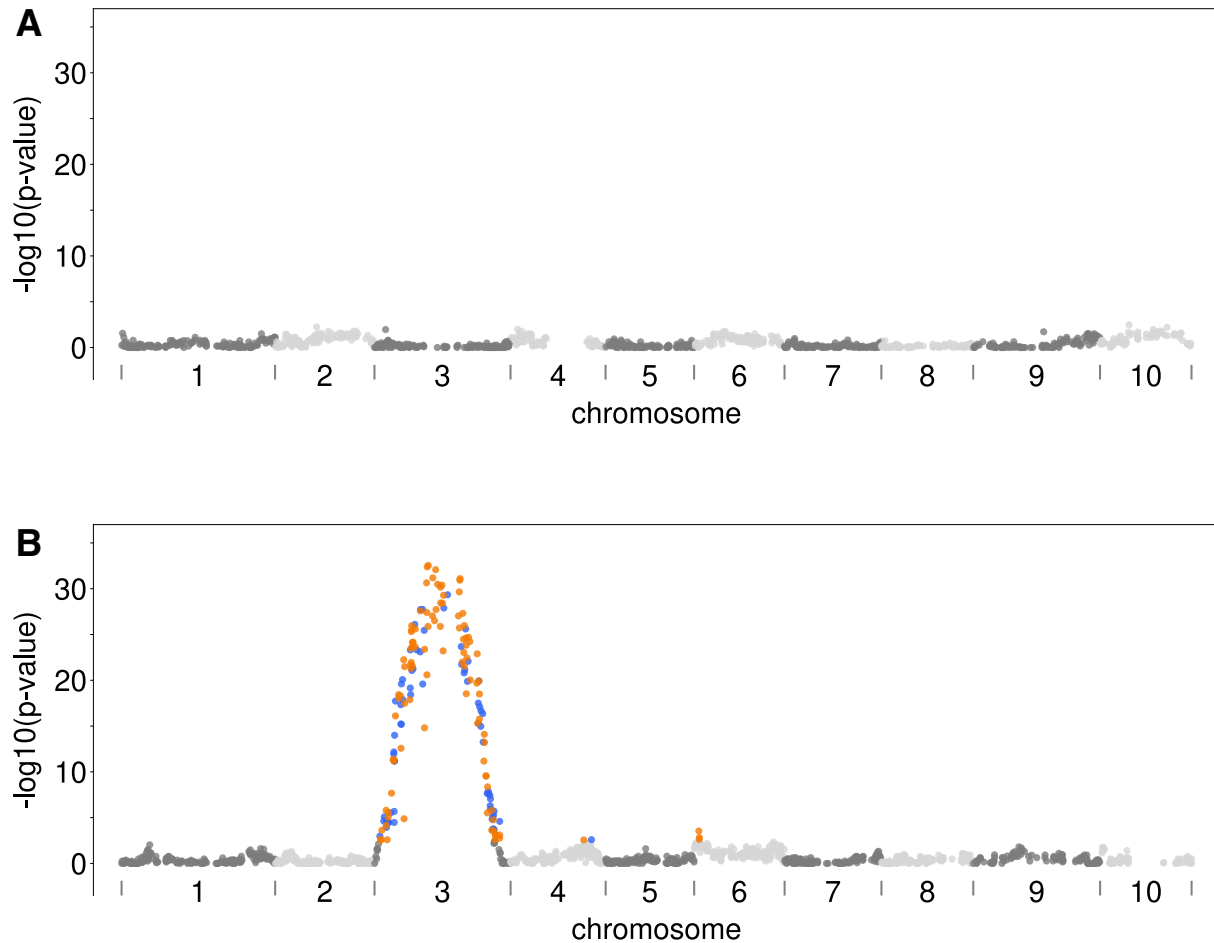


Fig. 3 Genome-wide association mapping of sex in the F1 progeny derived from a cross between Waka1 (P1: female) and Kita1 (P2: male) in *D. tokoro*. Manhattan plot of markers associated with sex phenotype as determined by Fisher's exact test with (A) P1-heterozygous marker set and (B) with P2-heterozygous marker set. Orange and blue dots indicate SNP and presence/absence markers, respectively, showing significant association with sex based on a 5 % false discovery rate ($q < 0.05$).

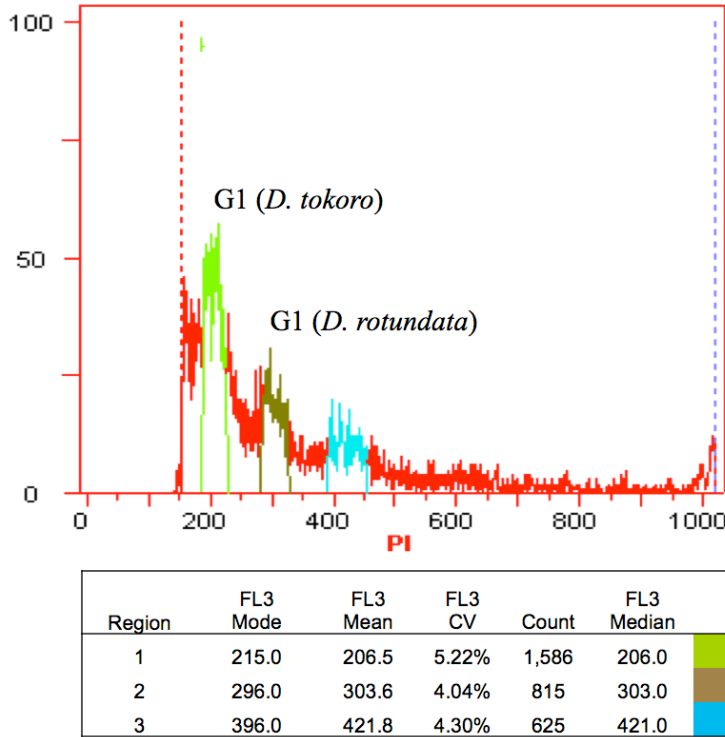


Fig. S1 Size estimation of *D. tokoro* genome by flow cytometry. Flow cytometry analysis was carried out using nuclei prepared from fresh leaf samples of a wild plant of *D. tokoro* collected in Kitakami, Iwate, Japan and a plant of *D. rotundata* maintained in a greenhouse at Iwate Biotechnology Research Center (IBRC). *D. rotundata* (570 Mb) was served as an internal reference standard of known genome size (Tamiru et al. 2017). Nuclei were isolated and stained with propidium iodide (PI) and analyzed using a Cell Lab QuantaTM SC Flow Cytometer (Beckman Coulter, USA) following the manufacturer's protocol. The ratio of G1 peak mean [*D. tokoro* (206.5): *D. rotundata* (303.6) = 0.680] was used to estimate the genome size of *D. tokoro* to be 388 Mb (570 Mb × 0.68).

Table S1. Summary of filtered ONT reads.

Number of reads (before filtering)	2,515,235 (3,126,676)
Total base-pairs (Gbp) (before filtering)	27.4 (32.7)
Genome coverage* (x)	70.6
Mean read length (kbp)	10.9
Longest fragment (kbp)	11.0
Shortest fragment (bp)	1
Accession No.	DRR344532

*Genome coverage is estimated from the expected genome size of *D. tokoro* (388 Mb).

Table S2. Summary of non-filtered Illumina short reads.

Sequence platform	Read length (bp)	Total base pairs(Gbp)	Genome coverage	Accession No.
Illumina MiSeq	35-251	24.6	63.4x	DRR344531
Illumina HiSeq 4000	150	37.8	97.4x	DRR347075
Total		62.4	160.8x	

Table S3. Number of male, female and non-flowering progeny derived from a Waka1 (P1) x Kita1 (P2) cross.

		Female	Male	Not flowered
Parent	Waka1 (P1)	1		
	Kita1 (P2)		1	
Progeny	186 individuals	38	89	59

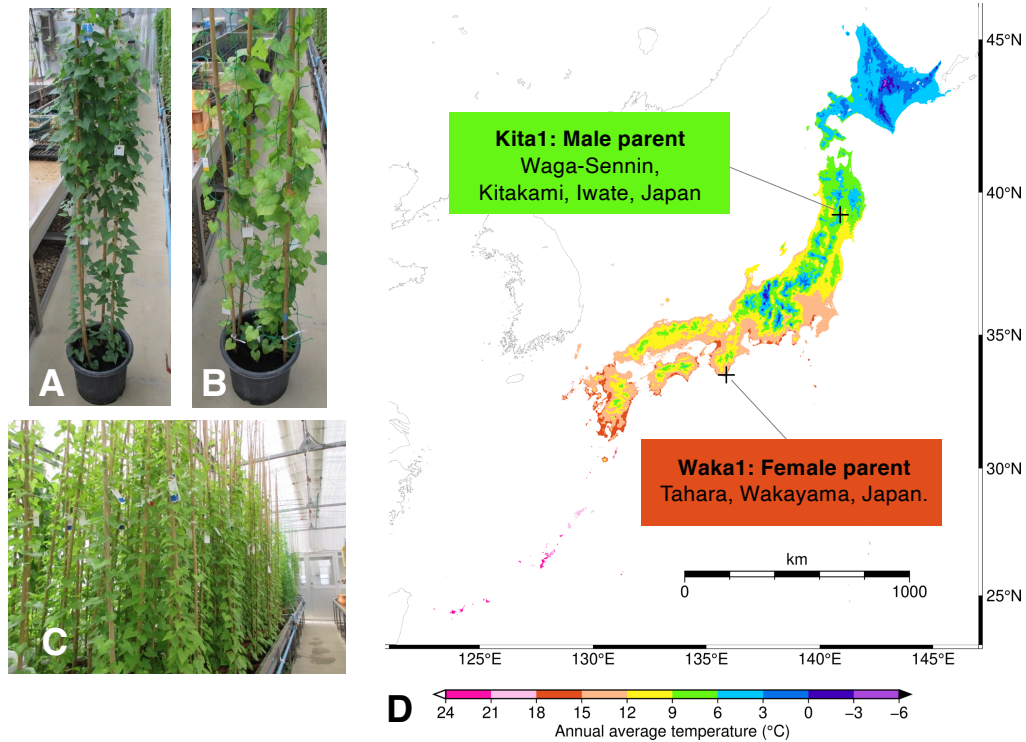


Fig. S2 *D. tokoro* plants used for a genetic cross and information of sites of origin. (A) A female individual Waka1. (B) A male individual Kita1. (C) Sideview of 186 F1 individuals obtained from a cross between Waka1 and Kita1. (D) Waka1 was collected from Tahara, Wakayama Pref. in the Kinki district of Japan. This place is close to the coast. The latitude and longitude are 33.538, 135.860, respectively, and the average annual temperature is 15-18°C. Kita1 was collected from Waga-Sennin in Kitakami, Iwate Pref. in the Tohoku district of Japan. This place is a mountainous. The latitude and longitude are 39.295, 140.896, respectively, and the average annual temperature is 6-9 °C. This map was created with GMT, Version 6.1.1 (Wessel et al. 2019). The annual average temperature on the map of Japan is drawn using "Annual average (climate) mesh data", downloaded from the National Land Numerical Information Download Service (JPGIS2.1) (<https://nlftp.mlit.go.jp/ksj/index.html>) published by the Ministry of Land, Infrastructure, Transport and Tourism.

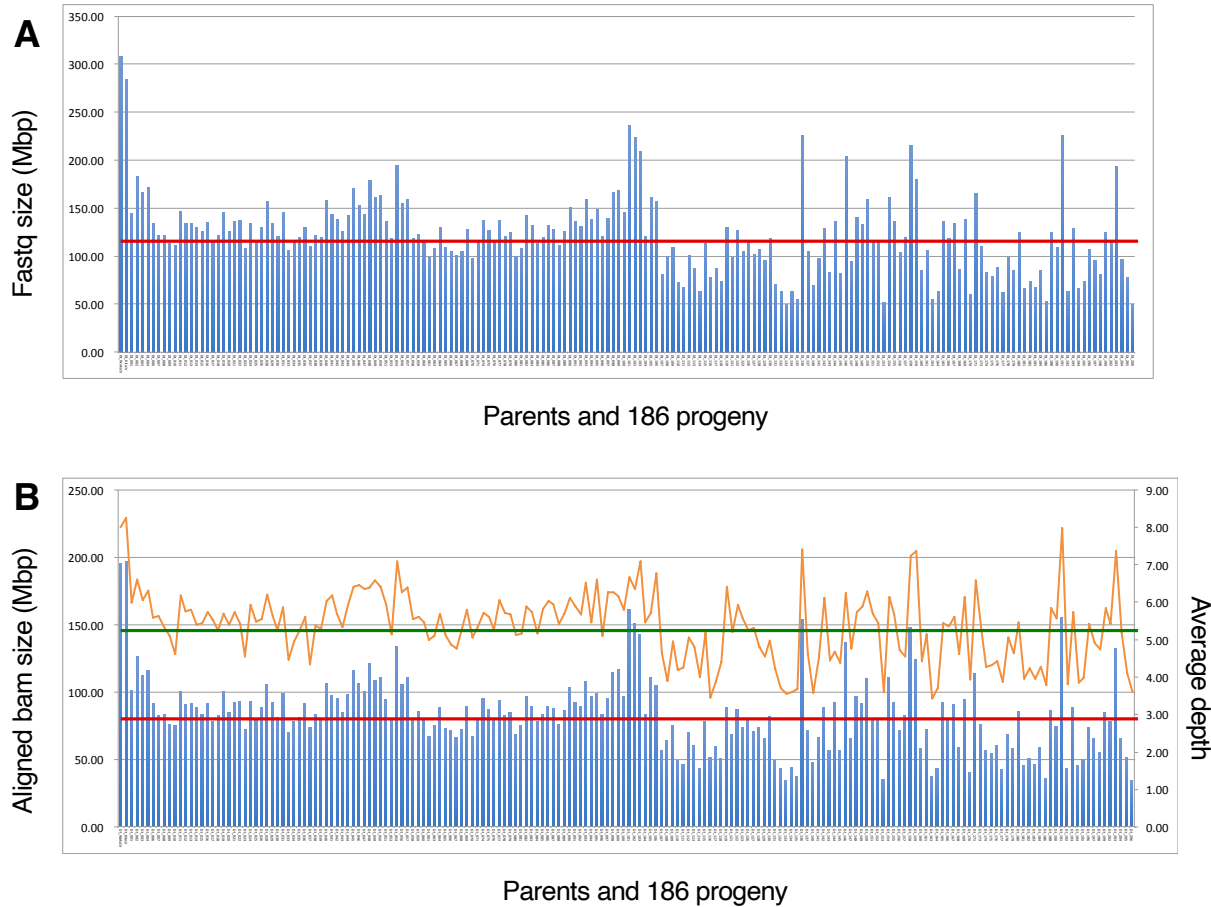


Fig S3 Summary of RAD tags generated for 186 F1 individuals derived from a cross between Waka1 (P1: female) and Kita1 (P2: male). In all graphs, the two bars on the left end indicate the parents Waka1 and Kita1, and the other indicate 186 F1 individuals. (A) The total size of filtered fastq of each individual (blue bars). The horizontal red line indicates the average fastq size of the progeny (120.7 Mbp). (B) Aligned bam size (blue bars) and average read depth at genomic regions in the reference genome aligned by the RAD-tags (orange line). The horizontal red line indicates the average aligned bam size of the progeny (82.3 Mbp), and the horizontal green line indicates the average read depth of the progeny (5.34 Mbp).

Table S4. Number of RAD markers used for anchoring the contigs after filtering.

Filtering step	Type	LG	SNP	PA	total
All RAD markers	testcross		5,894	5,071	10,965
Confirmed segregation ratio	P1-hetero		3,057	480	3,537
	P2-hetero		1,559	1,682	3,241
	(total)		4,616	2,162	6,778
Pruning and flanking	P1-hetero	49	988	181	1,169
	P2-hetero	55	768	881	1,649
	(total)		1,756	1,062	2,818
Anchoring contigs	P1-hetero	10	946	180	1,126
	P2-hetero	10	724	880	1,604
	(total)		1,670	1,060	2,730

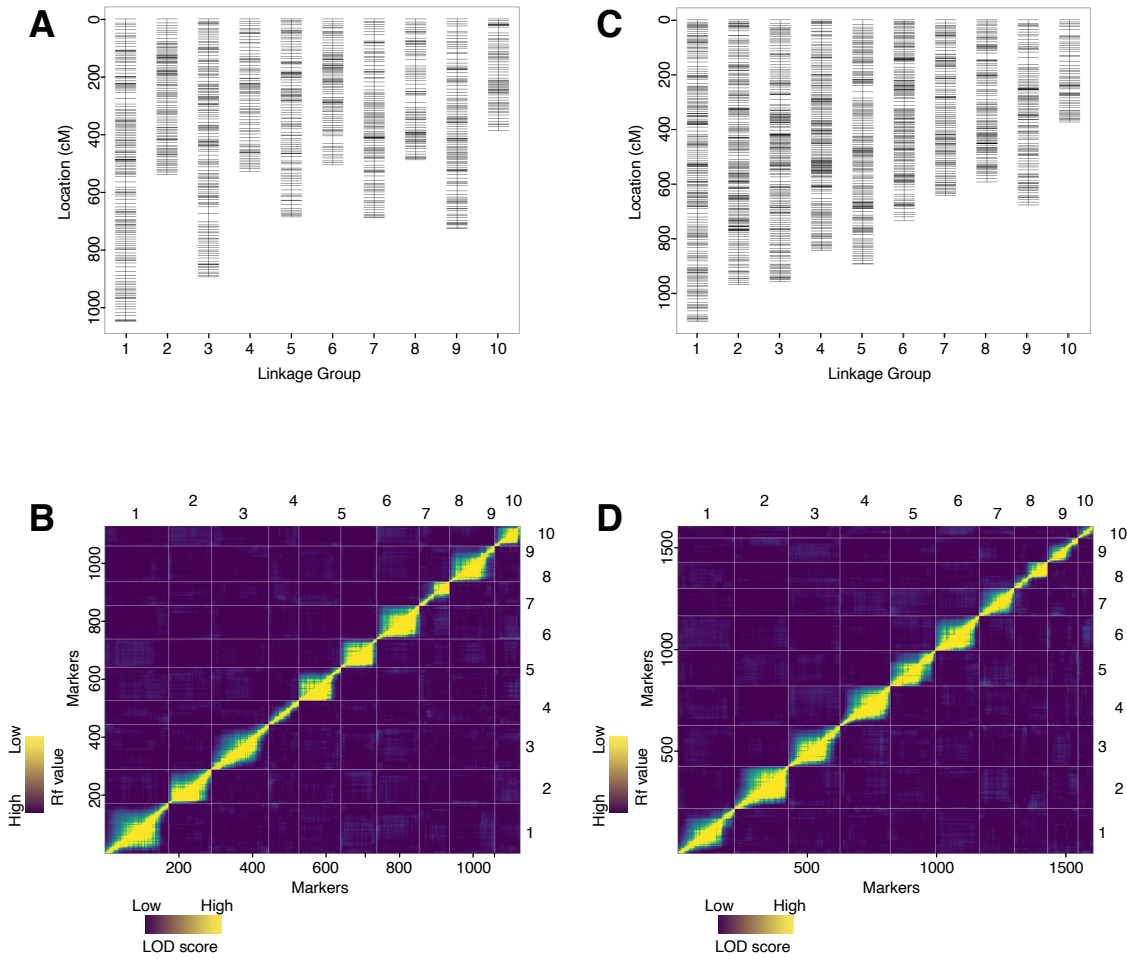


Fig. S4 RAD-seq-based linkage map of *D. tokoro* generated by the pseudo-testcross method using 186 F1 individuals. (A) P1-map generated using P1-heterozygous marker set. (B) Plots of estimated recombination fractions (upper-left triangle) and LOD score (lower-right triangle) for P1-Map. (C) P2-map generated using P2-heterozygous marker set. (D) Plots of estimated recombination fractions (upper-left triangle) and LOD score (lower-right triangle) for P2-Map. Yellow indicates linked (large LOD score or small recombination fraction) and blue indicates not linked (small LOD score or large recombination fraction).

		P2-map Linkage group									
		1	2	3	4	5	6	7	8	9	10
P1-map Linkage group	1	64	2	2	1	0	0	2	1	1	0
	2	2	52	1	0	0	2	2	0	0	1
	3	1	3	38	1	3	1	1	0	0	0
	4	1	1	0	51	1	0	0	1	0	0
	5	2	2	0	2	41	1	0	3	0	1
	6	3	1	2	0	1	38	0	1	0	0
	7	0	1	1	2	0	0	39	1	1	0
	8	2	0	1	1	0	1	0	30	0	0
	9	0	1	1	0	1	0	0	0	27	0
	10	0	3	0	1	1	0	2	0	2	17

Fig. S5. A matrix of the number of shared contigs between the P1-map and P2-map.
Both P1-Map and P2-Map contained 10 LGs.

Table S5. Summary of contigs anchored by RAD markers of the 10 linkage groups.

	P1 hetero	P2 hetero	P1 P2 total
Markers in 10 LGs	1,126	1,604	2,730
contig information anchored by marker:			
number	566	963	1,123
contig number %	19.3	32.9	38.3
contig total bps	303,270,609	320,556,813	378,798,395
contig total %	68.4	72.3	85.4

*The reference fasta size is 443,501,147 bp.

Table S6. Details of 18 RNA-seq samples.

No.	Organ	Phase	Sex	Stage*	Collected material	Fastq size
1	leaves		male		Kita1	1.71
2	stems		male		Kita1	1.35
3	root apex		male		Kita1	1.66
4	rhizome bud		male		Kita1	1.86
5	rhizome root		male		Kita1	1.61
6	rhizome stem		male		Kita1	1.79
7	rhizome storage		male		Kita1	1.78
8	shoot apex	vegetative	unknown		multiple wild	1.62
9	shoot apex	reproductive	female	0	multiple wild	1.87
11	shoot apex	reproductive	female	1	multiple wild	1.70
13	shoot apex	reproductive	female	2	multiple wild	1.81
10	shoot apex	reproductive	male	0	multiple wild	1.71
12	shoot apex	reproductive	male	1	multiple wild	1.74
14	shoot apex	reproductive	male	2	multiple wild	1.91
15	mature bud		female		multiple wild	1.85
16	mature bud		male		multiple wild	1.69
17	flower		female		multiple wild	1.83
18	flower		male		multiple wild	1.83
					total	31.17

*The reproductive shoot stage are indicated as follows. 0: shoot apical meristem (SAM), 1: inflorescence with unopened bracts, 2: inflorescences below 10 mm with unseparated bottom buds.

Supplementary Method

Identification of parental line-specific heterozygous RAD markers

Heterozygous SNP markers

SNP genotypes for P1, P2, and F1 progenies were obtained as a VCF file. The VCF file was generated as follows: (i) SAMtools v1.5 mpileup command with the option “-t DP,AD,SP -B -Q 18 -C 50”; (ii) BCFtools v1.5 call command with the option “-P 0 -v -m -f GQ,GP”; (iii) BCFtools view command with the options “-i ‘INFO/MQ≥40, INFO/MQ0F≤0.1, and AVG(GQ)≥10’”; and (iv) BCFtools norm command with the option “-m+any.” We rejected the variants with low read depth (< 10) or low genotype quality scores (< 10) in the two parents. Likewise, we regarded variants with low read depth (< 8) or low genotype quality scores (< 5) in F1 progenies as missing and only retained the variants with low missing rates (< 0.3). Subsequently, only bi-allelic SNPs were selected by the BCFtools view command with the option “-m 2 -M 2 -v snps”. Referring to the genotypes in the VCF file, heterozygous genotypes called by unbalanced allele frequency (out of 0.1-0.9 in F1 progenies) were regarded as missing, and filtering for missing rate (< 0.1) was applied again. As a result, 5,894 P1- or P2-heterozygous SNP markers were selected (shown as “All RAD markers” in Table S5). Next, a binomial test was performed to reject SNPs affected by segregating distortion in the F1 progenies. This binomial test assumes that the probability of success rate is 0.5 based on the two-side hypothesis, and we regarded variants having p-value less than 0.001 as segregation distortion. Finally, 3,057 P1-heterozygous SNP markers and 1,559 P2-heterozygous SNP markers were selected (shown as “Confirmed segregation ratio” in Table S5).

Heterozygous presence/absence RAD markers

The presence/absence markers were defined based on the alignment depth of parental line RAD-tags. A VCF file was generated to search for positions with contrasting read depth between the two parental plants P1 and P2 using the following commands: (i) SAMtools mpileup command with the option “-B -Q 18 -C 50”; (ii) BCFtools call command with the option “-A”; and (iii) BCFtools view command with the options “-i ‘MAX(FMT/DP)≥8 and MIN(FMT/DP)≤0’ -g miss -V indels”. This means that one of the parents (P1 or P2) has enough read depth (≥ 8) and another parent has no reads aligned on that region. Subsequently, we converted continuous positions in the VCF file to a feature that provides a region’s start and end coordinate information using the BEDTools v.2.26 merge command with the option “-d 10 -c 1 -o count”. We only retained sufficiently wide features (≥ 50 bp) in the BED file. Using the depth value in each feature given in

the BED file, presence/absence (PA) -based genotypes for parental plants P1 and P2 and F1 progenies were determined. For P1 and P2, we regarded genotypes having depth ≥ 4 as present genotypes, meaning the heterozygosity of presence and absence, while those having depth = 0 were classified as absent genotypes, meaning the homozygosity of absence. For F1 progenies, we classified markers with depth > 2 and = 0 as present and absent markers, respectively. Referring to the genotypes, heterozygous genotypes called by unbalanced allele frequency (out of 0.1-0.9 in F1 progenies) were rejected. As a result, 5,071 PA markers were selected (shown as “All RAD markers” in Table S5). Next, we applied the same binomial test for PA heterozygous markers as SNP-type heterozygous markers. Finally, 480 P1-heterozygous PA markers and 1,682 P2-heterozygous PA markers were selected (shown as “Confirmed segregation ratio” in Table S5).